Veterinary Microbiology 228 (2019) 134–142

Contents lists available at ScienceDirect

Veterinary Microbiology

journal homepage: www.elsevier.com/locate/vetmic

Cellular protein profiles altered by PRRSV infection of porcine monocytes-derived dendritic cells

Yue Hu[a,d,1], Xiangju Wu[a,1], Wenhai Feng[e], Feng Li[f], Zhao Wang[f,g,**], Jing Qi[a,c,***], Yijun Du[a,b,c,*]

[a] Shandong Key Laboratory of Animal Disease Control and Breeding, Institute of Animal Science and Veterinary Medicine, Shandong Academy of Agricultural Sciences, Sangyuan Road No. 8, Jinan 250100, China
[b] College of Veterinary Medicine, Qingdao Agricultural University, Qingdao 266109, China
[c] College of Life Science, Shandong Normal University, Jinan 250014, China
[d] Biotechnology Research Center, Shandong Academy of Agricultural Sciences, Jinan 250100, China
[e] State Key Laboratory of Agrobiotechnology, Department of Microbiology and Immunology, College of Biological Sciences, China Agricultural University, Beijing 100193, China
[f] Department of Biology and Microbiology, Department of Veterinary and Biomedical Sciences, South Dakota State University, Brookings, SD 57007, USA
[g] China Institute of Veterinary Drug Control, 8 Nandajie, Zhongguancun, Haidian, Beijing 100081, China

ARTICLE INFO

Keywords:
PRRSV
MoDCs
Cellular network
iTRAQ

ABSTRACT

Dendritic cells (DCs) are potent antigen-presenting cells (APCs) that play an important role in inducing primary antigen-specific immune responses. Some viruses have evolved to specifically target DCs to circumvent the host immune responses for their persistence in the host. One example is porcine reproductive and respiratory syndrome virus (PRRSV) that causes a persistent infection in pigs through modulating DC-mediated antiviral response. To study the cellular protein responses in PRRSV-infected monocyte-derived dendritic cells (MoDCs), two-dimensional liquid chromatography-tandem mass spectrometry coupled with isobaric tags for relative and absolute quantification (iTRAQ) labeling was employed to quantitatively identify the differentially expressed proteins in PRRSV-infected MoDCs and the control cells. A total of 252 cellular proteins in MoDCs that were significantly altered at different time periods post-infection were identified. Differentially expressed proteins that are involved in the endocytosis pathway, actin cytoskeleton network, antigen processing and presentation, JAK-STAT signaling pathway and PRRSV receptors were identified and further analyzed. Among them, the expression changes of STAT1, Mx1, PICALM and SLA-DR were further verified by Western blotting. The protein profiles associated with PRRSV infection of MoDCs should offer novel insights to further investigation of PRRSV-mediated antiviral evasion mechanism and its pathobiology in swine.

1. Introduction

Porcine reproductive and respiratory syndrome virus (PRRSV) is a pathogen that causes significant economic impacts on the swine industry worldwide (Lu et al., 2012). The virus is an enveloped positive-strand RNA virus that together with the equine arteritis virus, lactate dehydrogenase-elevating virus, and simian hemorrhagic fever virus belong to the *Arteriviridae* family (Meulenberg, 2000). PRRS virus switches its genome into double-strand RNA (dsRNA) in infected cells during replication (Duan et al., 1997; Lawson et al., 1997). PRRSV has a very restricted host specificity and cell tropism, which can grow in primary cultures of pulmonary alveolar macrophages (PAMs), African green monkey kidney cells or derivatives (CL2621 or MARC-145 cells) and MoDCs *in vitro* (Shi et al., 2015). The hallmarks of PRRS include poor antiviral immune response and persistent infection in pigs (Butler et al., 2014).

DCs are a heterogeneous group of potent APCs with the unique capacity to prime naive T-cell responses. MoDCs and bone marrow-derived DCs (BMDCs) are DCs generated *in vitro*. MoDCs have more advantages and more versatile applications than BMDCs, since they can

* Corresponding author at: Shandong Key Laboratory of Animal Disease Control and Breeding, Institute of Animal Science and Veterinary Medicine, Shandong Academy of Agricultural Sciences, Sangyuan Road No. 8, Jinan 250100, China.
** Corresponding author at: China Institute of Veterinary Drug Control, 8 Nandajie, Zhongguancun, Haidian, Beijing 100081, China.
*** Corresponding author at: Shandong Key Laboratory of Animal Disease Control and Breeding, Institute of Animal Science and Veterinary Medicine, Shandong Academy of Agricultural Sciences, Sangyuan Road No. 8 Jinan 250100, China.
E-mail addresses: zhaowang2007@outlook.com (Z. Wang), qj-happy2008@163.com (J. Qi), duyijun0916@163.com (Y. Du).
[1] These authors contributed equally to this article.

https://doi.org/10.1016/j.vetmic.2018.11.016
Received 27 August 2018; Received in revised form 14 November 2018; Accepted 16 November 2018

be largely generated without sacrificing the animal and be in an immature state, which facilitates studying DCs maturation in response to virus infection or others (Summerfield and McCullough, 2009). PRRSV is able to replicate in MoDCs (Shi et al., 2015), however, little is known about the cellular protein profiles in MoDCs in response to PRRSV infection.

iTRAQ is employed widely, with a proven value in discovery-based proteomics. iTRAQ allows for simultaneous protein identification and relative quantification obtained at the MS/MS level from peptide fragments and low mass reporter ions, respectively. iTRAQ has been widely used to study cellular protein profiles associated with virus infections, such as Hepatitis C virus (HCV), rabies virus, J Avian leukosis virus (ALV-J), porcine epidemic diarrhea virus (PEDV), foot-and-mouth disease virus (FMDV), PRRSV and porcine circovirus type 2 (PCV2) (Lu et al., 2012; Ye et al., 2015; Zeng et al., 2015; Guo et al., 2016; Zhu et al., 2015; Yang et al., 2015; Li et al., 2015a; Liu et al., 2013). In this study, we described a quantitative proteomic analysis of MoDCs infected with PRRSV using the multiplex capability of the iTRAQ approach. A total of 1756 protein candidates were identified in association with PRRSV infection, of which, 1090 proteins contain at least two unique peptides. There were 252 proteins showed significantly alterd expressions ($p \leq 0.05$ and more than 1.5-fold change) at different post-infection times. Besides, all the identified proteins were subjected to bioinformatic analysis by using the Gene Ontology (GO) database, the Kyoto Encyclopedia of Genes and Genomes (KEGG) database and the Cluster of Orthologous Groups of proteins (COG) database to identify the protein networks involved in the PRRSV lifecycle. Furthermore, function enrichment analysis (GO enrichment and KEGG enrichment) of these differentially expressed proteins showed enrichment in several biological pathways, which likely play important roles in PRRSV replication in porcine MoDCs.

2. Material and methods

2.1. Virus and preparation of porcine peripheral blood MoDCs

The 10th-passage of HP-PRRSV SY0608 (GenBank: EU144079) strain (Li et al., 2007) was propagated and titrated in MARC-145 cells. The titer of the virus stock was $10^{7.1}$ $TCID_{50}$/ml.

Blood samples were collected from four 6-week-old healthy crossbred pigs, which were obtained from a local farm without PRRSV, PCV2, porcine parvovirus (PPV), pseudorabies virus (PRV) and actinobacillus pleuropneumoniae (APP) history. All pigs were tested and proven to be seronegative for PRRS by indirect enzyme-linked immunosorbent assay (iELISA) and PRRSV negative by RT-PCR. MoDCs were isolated and cultured as described previously (Hu et al., 2016). After 6 days, MoDCs were used for PRRSV infection.

2.2. Virus inoculation

The MoDCs were inoculated with HP-PRRSV SY0608 strain at an MOI of 1 and collected at 12, 24 and 36 hours post inoculation (hpi). The uninfected cells served as mock-infected cells. Viral propagation was confirmed by real time RT-PCR and Western blotting with an in-house made monoclonal antibody against PRRSV-N protein.

2.3. Overview of the experimental design

In this study, the main objective was to identify the differential expression of proteins between PRRSV-infected MoDCs and mock-infected MoDCs. The PRRSV-infected MoDCs and mock-infected MoDCs were prepared for comparative proteomic analysis. An overview of the iTRAQ experimental design in three biological replicates is shown in Fig. 1. Proteins were extracted from the cells for eighteen samples, which were divided into 6 groups: 12 h mock-infected MoDCs, iTRAQ 113; 24 h mock-infected MoDCs, iTRAQ 114; 36 h mock-infected MoDCs, iTRAQ 115; 12 h PRRSV-infected MoDCs, iTRAQ 116; 24 h PRRSV-infected MoDCs, iTRAQ 117; 36 h PRRSV-infected MoDCs, iTRAQ 118. For Western blotting and real time RT-PCR, the experimental design is the same with the proteomic analysis, every sample was repeated in three technique replicates. β-actin was used as an internal control to normalize the quantitative data.

2.4. Protein extraction, digestion, iTRAQ labeling and fractionation

Cells were collected with 300 µl of lysis buffer (7 M urea, 2 M thiourea, 2% (w/v) CHAPS) containing a complete protease inhibitor cocktail (Sigma-Aldrich, St. Louis, MO, USA) at 12, 24 and 36 hpi. Protein extraction was performed following a previous report (Liu et al., 2016). After reduction and alkylation as described in the iTRAQ protocol (AB Sciex, Dublin, CA, USA), protein solutions were digested overnight at 37 °C with sequence grade modified trypsin (Promega, Madison, USA) and then labeled with the different iTRAQ tags (Fig. 1). All of the labeled samples were mixed with equal total protein amount and were fractionated using high-performance liquid chromatography (HPLC) system (Thermo DINOEX Ultimate 3000 BioRS) equipped with a Durashell C18 (5 µm, 100 Å, 4.6 × 250 mm). At last, 12 fractions were collected.

2.5. LC–MS/MS analysis

LC–MS/MS analysis was performed on an AB SCIEX nanoLC-MS/MS (Triple TOF 5600 plus) system. Samples were chromatographed using a 90 min gradient from 2 to 30% (buffer A 0.1% (v/v) formic acid, 5% (v/v) acetonitrile, buffer B 0.1% (v/v) formic acid, 95% (v/v) acetonitrile) after direct injection onto a 20 µm PicoFrit emitter packed to 12 cm with Magic C18 AQ 3 µm 120 Å stationary phase. MS1 spectra were collected in the range 350–1500 *m/z* for 250 ms. The 20 most intense precursors with charge state 2–5 were selected for fragmentation, and MS2 spectra were collected in the range 50–2000 *m/z* for 100 ms; precursor ions were excluded from reselection for 15 s.

2.6. Data analysis

The original MS/MS file data were submitted to Protein Pilot Software v4.5 for data analysis. For protein identification, the Paragon algorithm that was integrated into Protein Pilot was employed against uniprot Sus scrofa database (34,242 items) for database searching. The parameters were set according to the method described previously (Zhang et al., 2018). For protein abundance ratios measured using iTRAQ, we took a 1.5-fold change as the threshold and a corrected $p \leq 0.05$ to identify significant changes.

2.7. Bioinformatics

To determine the biological and functional properties of all the identified proteins, identified protein sequences were mapped with Gene Ontology (GO) Terms (http://geneontology.org/) with blast2go. Clusters of Orthologous Groups of Proteins System (https://www.ncbi.nlm.nih.gov/COG/) was employed for the functional annotation of genes from new genomes and for research into genome evolution. To identify candidate biomarkers, we employed hypergeometric test to perform GO enrichment and KEGG pathway enrichment with our in-home program. A *p*-value ≤ 0.05 was used as the threshold to determine the significant enrichments identified by the GO and KEGG pathways (Yang et al., 2018). The protein-protein interaction network was analyzed by Search Tool for the Retrieval of Interacting Genes (STRING) database (http://string.embl.de/).

2.8. Western blotting

The protein concentration of each sample was determined by BCA

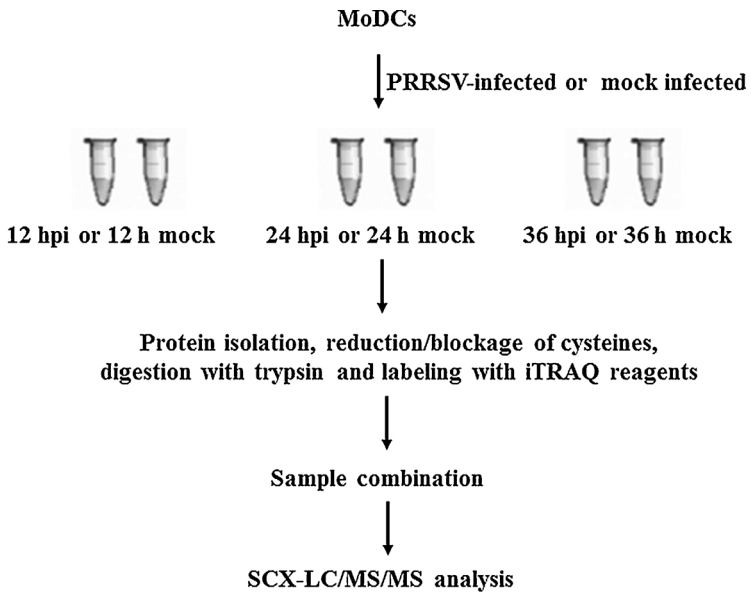

Fig. 1. Strategy for iTRAQ-coupled two-dimensional liquid chromatography-tandem mass spectrometry (2D LC–MS/MS) analysis of MoDCs infected with PRRSV. Three biological replicates were performed in this study. 12 h mock (Repeat 1-Repeat 3); 24 h mock (Repeat 1-Repeat 3); 36 h mock (Repeat 1-Repeat 3); 12 hpi (Repeat 1-Repeat 3); 24 hpi (Repeat 1-Repeat 3); 36 hpi (Repeat 1-Repeat 3).

iTRAQ group	iTRAQ 113	iTRAQ 114	iTRAQ 115	iTRAQ 116	iTRAQ 117	iTRAQ 118
Sample 1	12 h mock-1	24 h mock-1	36 h mock-1	12 hpi-1	24 hpi-1	36 hpi-1
Sample 2	12 h mock-2	24 h mock-2	36 h mock-2	12 hpi-2	24 hpi-2	36 hpi-2
Sample 3	12 h mock-3	24 h mock-3	36 h mock-3	12 hpi-3	24 hpi-3	36 hpi-3

protein assay kit (Pierce Biotechnology, Rockford, USA). The cell lysates were analyzed by sodium dodecyl sulfate-polyacrylamide gel electrophoresis (SDS-PAGE) and Western blotting analysis. Briefly, equivalent amounts of cell lysates (8 μg) were subjected to 12% SDS-PAGE gels and then transferred to PVDF transfer membranes (Millipore, Billerica, USA). After blotting, the membranes were incubated at 37 °C for 60 min with rabbit polyclonal antibody (pAb) to STAT1 (Cell Signaling, Danvers, USA), mouse monoclonal antibody (mAb) to Mx1 (Abcam, Cambridge, UK), pAb to PICALM (Novus, Littleton, USA), mAb to SLA-DR (Abcam, Cambridge, UK), mAb to N protein of PRRSV (in-house made) or β-actin antibody (Santa Cruz Biotechnology, Santa Cruz, USA), respectively. After washing three times with 0.05% TBST, the membranes were incubated at 37 °C for 60 min with horseradish peroxidase (HRP)-conjugated goat anti-rabbit IgG or goat anti-mouse IgG (Boster, Wuhan, China). The membranes were developed using SuperSignal West Pico Chemiluminescent Substrate according to the manufacturer's suggestions (Pierce, Rockford, IL, USA). Digital signal acquisition and analysis were conducted by the Molecular Imager® ChemiDoc™ XRS + systems with lmageLab™ software (Bio-Rad, California, USA). β-actin was used as an internal control to normalize the quantitative data.

2.9. Real time RT-PCR

To determine the mRNA expression of PRRSV-N in MoDCs, real-time RT-PCR was carried out. Total RNA was extracted from 1×10^6 MoDCs collected at 12, 24 and 36 hpi using TRIzol reagent (Invitrogen, Carlsbad, USA) according to the manufacturer's protocol. 20 μl of cDNA was obtained after reverse transcription of 1 μg RNA using Primer Script™ RT Reagent Kit with gDNA Eraser (Perfect Real Time) (Takara Co., Ltd., Japan) following instructions given by the manufacturer. 1 μl cDNA was subsequently used for SYBR green PCR assay (Applied Biosystems, USA) as previously described (Du et al., 2014a), using the following primers: PRRSV-N sense primer: 5′-AATAACAACGGCAAGC AGCAG-3′ and antisense primer: 5′−CCTCTGGACTGGTTTTGTTGG-3′; β-actin sense primer: 5′-TCTGGCACCACACCTTCT-3′ and antisense primer: 5′- GATCTGGGTCATCTTCTCAC-3′. The abundance of PRRSV-N mRNA in each sample was assayed three times and normalized to that of β-actin mRNA.

2.10. Statistical analysis

Data were compared and the differences were determined by One-way repeated measurement ANOVA and Least significance difference (LSD). A p-value < 0.05 was considered statistically significant (Du et al., 2014b).

3. Results

3.1. Confirmation of PRRSV propagation in MoDCs by real time RT-PCR and Western blotting

To confirm that PRRSV could propagate in MoDCs, the cellular mRNA and proteins were extracted from PRRSV-infected MoDCs and mock-infected MoDCs. Real time RT-PCR and Western blotting revealed that both the mRNA and protein levels of PRRSV-N were detected at 12, 24 and 36 hpi in PRRSV-infected MoDCs but not in mock-infected MoDCs, and the mRNA and protein levels of PRRSV-N were gradually increased in PRRSV-infected MoDCs from 12 to 36 hpi (Fig. 2A, B), respectively, indicating that PRRSV could propagate in MoDCs. The mRNA levels of PRRSV-N in mock-infected MoDCs were undetectable (data not shown). We also found that about 30%, 55% and 65% of the cells were infected at 12, 24 and 36 hpi, respectively, as evidenced by flow cytometry analysis with monoclonal antibody against PRRSV-N

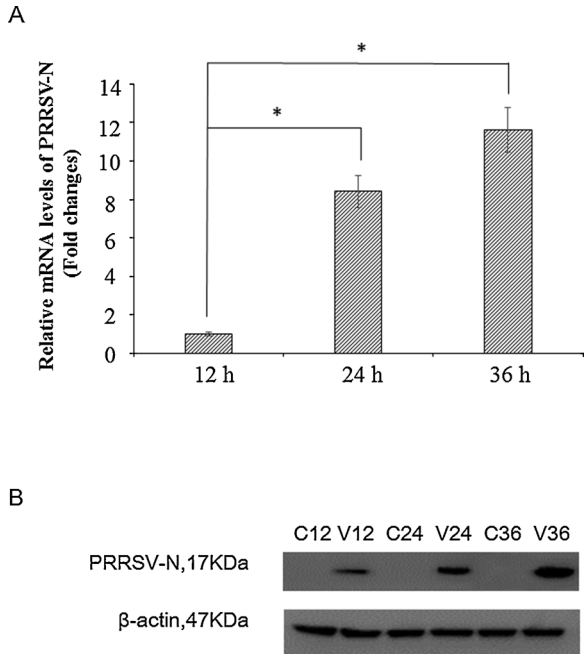

Fig. 2. mRNA and protein levels of PRRSV-N in MoDCs were examined by real time RT-PCR and Western blotting assay, respectively. (A) The relative mRNA levels of PRRSV-N in PRRSV-infected MoDCs and mock-infected MoDCs were detected by real time RT-PCR. Total RNA of PRRSV-infected MoDCs were extracted at 12, 24 and 36 hpi. Relative mRNA levels of PRRSV-N were shown as fold changes relative to the PRRSV-infected MoDCs at 12 hpi. The data represent the means of three independent experiments, with each experiment performed in triplicate. Error bars indicate the standard deviations of three independent experiments. * means significant difference ($p < 0.05$). (B) The protein levels of PRRSV-N in PRRSV-infected MoDCs and mock-infected MoDCs detected by Western blotting. β-actin was used as an internal control to normalize the quantitative data. The data presented here were results from one experiment of three Western blotting experiments. V12, V24 and V36 mean 12 h, 24 h and 36 h after PRRSV infection. C12, C24 and C36 mean 12 h, 24 h and 36 h after mock infection.

protein (data not shown).

3.2. Protein profile by iTRAQ-coupled 2D LC–MS/MS analysis

Protein extracts were individually prepared from both PRRSV-infected and mock-infected MoDCs at 12, 24 and 36 hpi. 1756 proteins were detected by iTRAQ-coupled 2D LC–MS/MS analysis and 252 proteins displayed significantly altered expression levels between PRRSV-infected and mock-infected MoDCs at different times post-infection as shown in Supplementary Fig. 1 and Supplementary Table 1 ($p \leq 0.05$ and ratios ≥ 1.5 or ≤ 0.67), in which they were divided into 4 different clusters: up-regulation (180 proteins), down-regulation (59 proteins), up-down-regulation (6 proteins) and down-up-regulation (7 proteins). The up-regulation cluster means the expression of the proteins was significantly up-regulated at 12, 24 or 36 hpi. The down-regulation cluster means the expression of the proteins was significantly down-regulated at 12, 24 or 36 hpi. The up-down-regulation cluster means the expression of the proteins was significantly up-regulated at 12 or 24 hpi, and then significantly down-regulated at 24 or 36 hpi. The down-up-regulation cluster means the expression of the proteins was significantly down-regulated at 12 or 24 hpi, and then significantly up-regulated at 24 or 36 hpi.

In term of GO database, the differentially expressed proteins were divided into Biological Process (BP), Cellular Component (CC) and Molecular Function (MF). Among the 180 up-regulation proteins, there were 131 BP, 30 CC, and 25 MF. Specially, cellular process was highly represented in BP, organelle was highly represented in CC, and oxidoreductase activity was highly represented in MF (Supplementary Fig. 2A). Among the 59 down-regulation proteins, there were 56 BP, 1 CC, and 13 MF (Supplementary Fig. 2B). Among the 6 up-down-regulation proteins, there were 5 BP, 3 CC, and 0 MF (Supplementary Fig. 2C), and among the 7 down-up-regulation proteins, 28 BP, 7 CC, and 4 MF were included (Supplementary Fig. 2D).

In the term of KEGG pathway analysis, the up-regulation proteins participated in 14 pathways, the down-regulation proteins participated in 6 pathways, the up-down-regulation proteins participated in 5 pathways, and the down-up-regulation proteins participated in 4 pathways (Fig. 3). Among the significantly differentially expressed proteins, TfR, dynamin, clathrin, AP2, cPML, Hsc70, Dab2 and UBPY were enriched in the endocytosis pathway (Supplementary Fig. 3A), while IQGAP, ERM, F2RCD14, FN1, ITG, PI3K, Arp2/3 and GSN were enriched in the regulation of actin cytoskeleton (Supplementary Fig. 3B). In addition, Hsp70, BRp57, CALR and MHC II were enriched in antigen processing and presentation (Supplementary Fig. 3C). Four other proteins including SHP1, STAT, GRB and PI3K were enriched in JAK-STAT signaling pathway (Supplementary Fig. 3D).

Numerous antiviral proteins such as OAS, Mx1 and Mx2 were significantly up-regulated after PRRSV infection. Interestingly, we noticed that Vimentin and CD163, which serve as receptors for PRRSV, expressed differently over the course of viral infection in MoDCs (Van et al., 2010; Zhang and Yoo, 2015). Specifically, Vimentin was significantly up-regulated at 24 hpi, while CD163 was significantly up-regulated at 12 hpi and down-regulated at 36 hpi (Supplementary Table 1).

In the term of COG analysis, 252 proteins were sub-categorized into 20 COG classifications, and the classification O (posttranslational modification, protein turnover, chaperones) was the most highly represented (Fig. 4).

3.3. Validation of changes in protein levels by Western blotting analysis

In order to further validate the differentially expressed proteins identified by the iTRAQ labeled 2D LC–MS/MS system, we selected the protein STAT1, Mx1, PICALM and SLA-DR for Western blotting analysis. Equal amounts of cell lysates from PRRSV-infected MoDCs and mock-infected MoDCs were tested with antibodies to STAT1, Mx1, PICALM and SLA-DR, respectively. As shown in Fig. 5, the expressions of STAT1, PICALM and SLA-DR were obviously increased in PRRSV-infected MoDCs when compared with mock-infected MoDCs at 12 hpi. The expression of Mx1 was significantly induced and gradually increased in PRRSV-infected MoDCs from 12 hpi to 36 hpi. These data were consistent with those obtained from the iTRAQ-coupled 2D LC–MS/MS analysis, thereby validating the findings of our approach.

3.4. Protein-protein interaction analysis

The network of significantly differentially expressed proteins of PRRSV-infected MoDCs ($p \leq 0.05$ and ratios ≥ 1.5 or ≤ 0.67) was analyzed by STRING software, of which, 54 items were shown successfully (Fig. 6). There were two regions focusing on more proteins, which was circled in red and boxed in black, respectively. The group circled in red contains Vimentin, SLA-DRA, CLTC, Mx1, Mx2, STAT1, PICALM and GRB2. Interestingly, proteins in this group were all up-regulated after PRRSV infecting MoDCs. The group boxed in black contains RPL3, RPL4, RPL6, RPL13 A, EIF3G, EEF1A and KARS, of which, RPL13 A, EIF3G and KARS were down-regulated, while RPL3, RPL4, RPL6 and EEF1A were up-regulated following PRRSV infection in MoDCs (Fig. 6 and Supplementary Table 1).

4. Discussion

DCs are recognized as the most effective APCs, which capture and process antigens, display large amounts of MHC–peptide complexes at

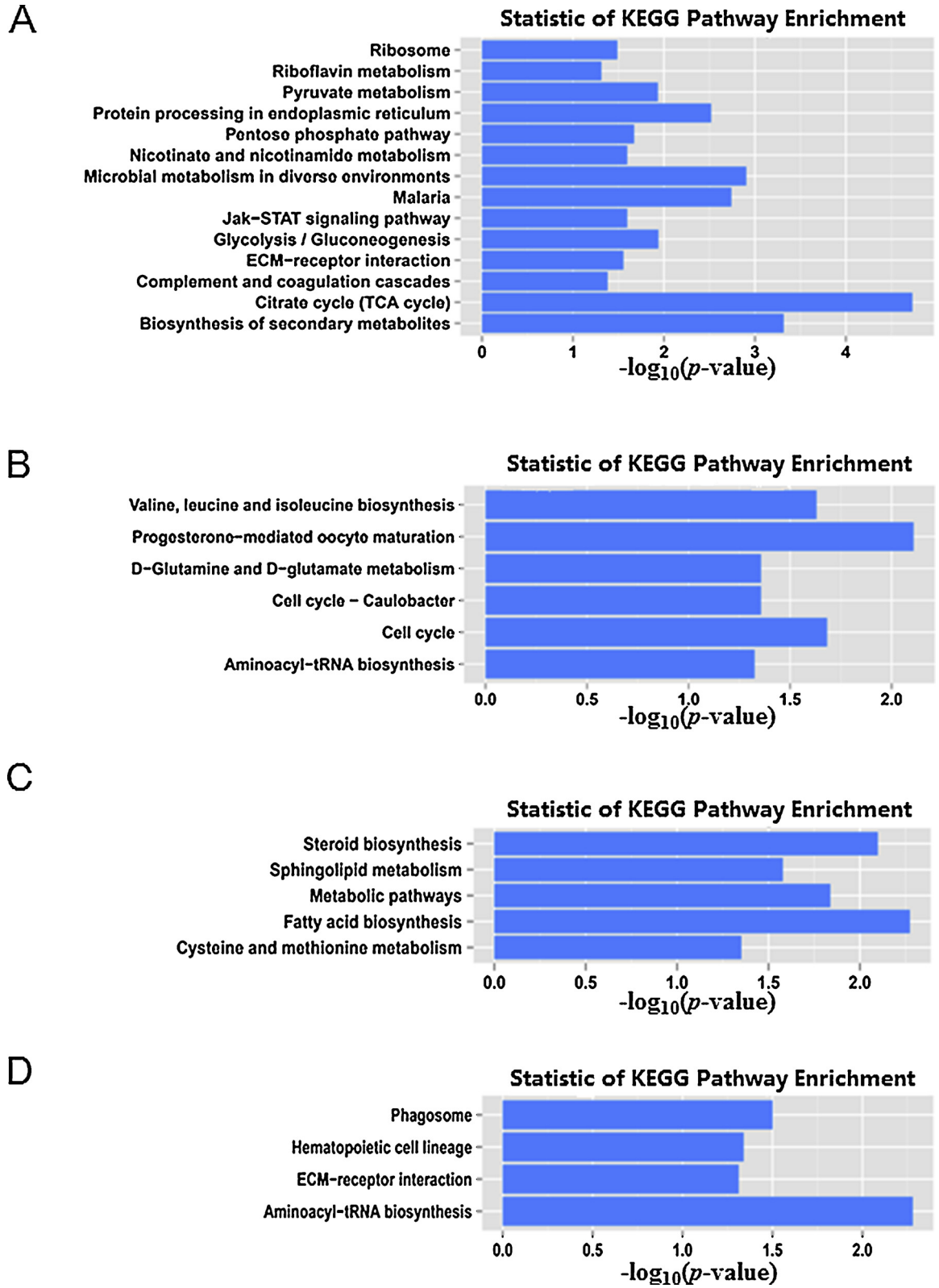

Fig. 3. Statistic of KEGG pathway enrichment. (A) Statistic of KEGG pathway enrichment on up-regulation proteins. (B) Statistic of KEGG pathway enrichment on down-regulation proteins. (C) Statistic of KEGG pathway enrichment on up-down-regulation proteins. (D) Statistic of KEGG pathway enrichment on down-up-regulation proteins. The *p*-values were shown for each pathway based on hypergeometric distribution.

their surface, and then present antigens to T cells for the induction of immunity. Moreover, DCs are also critical for bridging the innate and the adaptive immune response (Banchereau and Steinman, 1998).

PRRSV is unique in that it causes severe clinical disease, while maintains a persistent infection up to 200 days. Infecting and long-term replicating in MoDCs by PRRSV may lead to this phenotype (Chand et al., 2012). It is suggested that MoDCs are both target cells and effector cells during host response to PRRSV infection. Understanding the

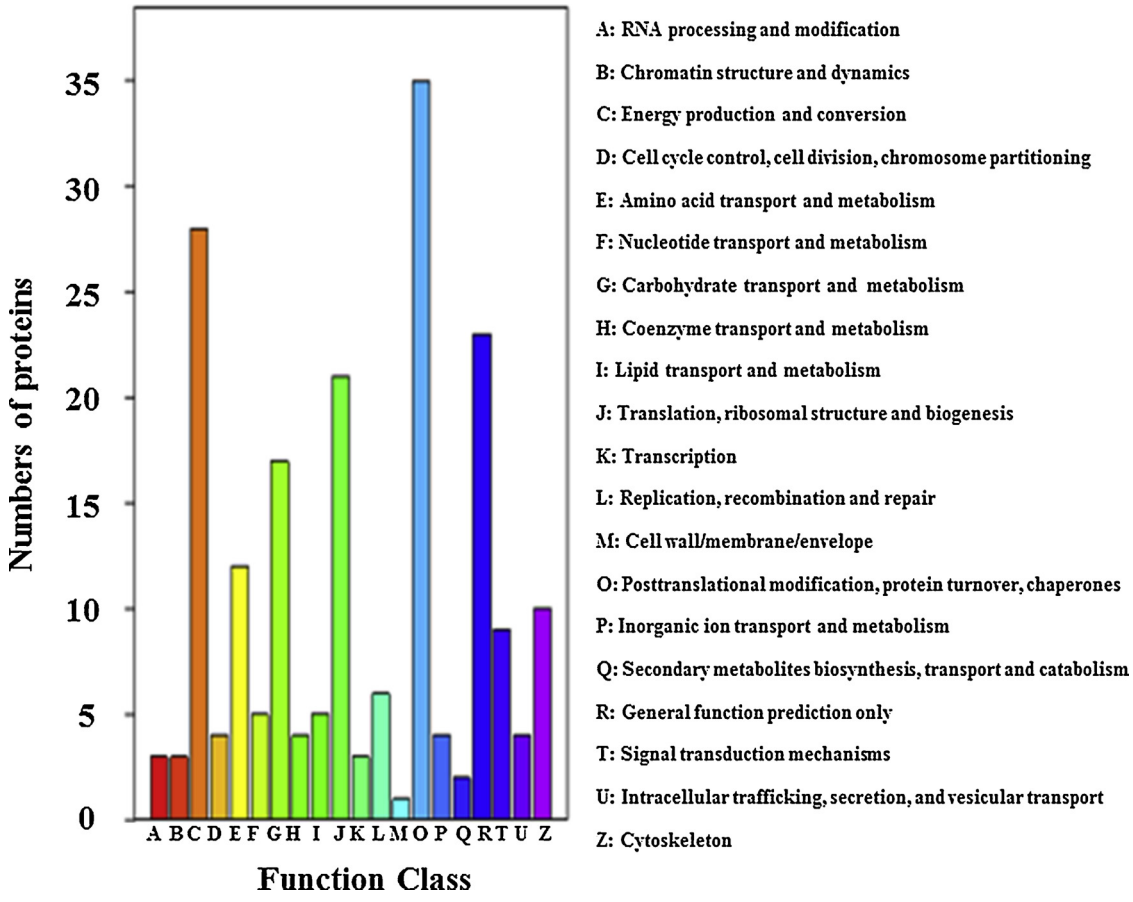

Fig. 4. COG function classification of all identified proteins. The x-axis indicated different classifications and the y-axis indicated the number of proteins in COG class.

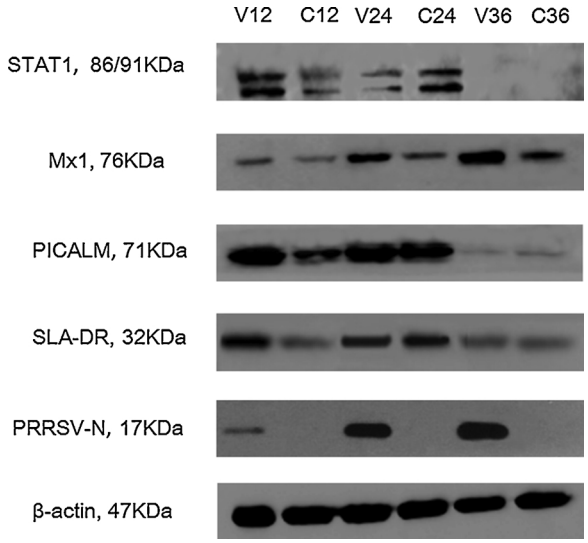

Fig. 5. Confirmation of four differentially expressed proteins (STAT1, Mx1, PICALM and SLA-DR) and N protein of PRRSV in PRRSV-infected and mock-infected MoDCs by Western blotting. β-actin was used as an internal control to normalize the quantitative data. The data presented here were results from one experiment of three Western blotting experiments.

interactions between PRRSV and MoDCs is critical for elucidating PRRSV pathogenesis and the immunologic mechanism. In this study, proteins associated with endocytosis, regulation of actin cytoskeleton, antigen processing and presentation, JAK-STAT signaling pathway, antiviral and PRRSV receptors of MoDCs were found and analyzed.

As we know, clathrin is a protein that plays a major role in the formation of coated vesicles, and clathrin-mediated endocytosis is the uptake of material into the cell from the surface using clathrin-coated vesicles. Clathrin-dependent endocytosis (often referred to as receptor-mediated endocytosis) is one of the basic molecular machineries of the endocytosis pathway (Lemire et al., 2012; Bonazzi and Cossart, 2006). Lots of cargoes modulate the functions of antigen-presenting cells via clathrin-mediated endocytosis (Lemire et al., 2012). In this study, the clathrin associated protein clathrin heavy chain (CLTC), clathrin light chain (CLTA), phosphatidylinositol binding clathrin assembly protein (PICALM) and adaptor 2 protein (AP2) were successfully identified by iTRAQ technology (McMahon and Boucrot, 2011; Tebar et al., 1999), which were all significantly increased in PRRSV-infected MoDCs at different hours post-infection (Supplementary Fig. 3A and Supplementary Table 1). PICALM expression in MoDCs with PRRSV infection or mock infection was confirmed by Western blotting (Fig. 5). However, proteins associated with clathrin-independent endocytosis were not significantly changed. In addition, two previously reported PRRSV receptors, vimentin and CD163 were successfully identified in our study (Van et al., 2010; Zhang and Yoo, 2015). The expressions of vimentin and CD163 were significantly up-regulated after PRRSV infecting MoDCs (Supplementary Table 1). We speculate that PRRSV enters into MoDCs via clathrin-dependent endocytosis and the increased expression of PRRSV receptors vimentin and CD163 likely facilitates PRRSV enter into and replicate in MoDCs, which warrant further investigation.

The function of DC antigen capture and presentation could be affected by DC actin cytoskeleton remodeling (West et al., 2004; Comrie et al., 2015). For example, endocytosis in DCs was impaired for actin cytoskeleton rearrangements influenced by PCV2 DNA (Balmelli et al., 2011). Intact cytoskeleton is essential for DC-mediated HIV-1 transmission to $CD4^+$ T cells (Wang et al., 2008). In this study, 8 proteins

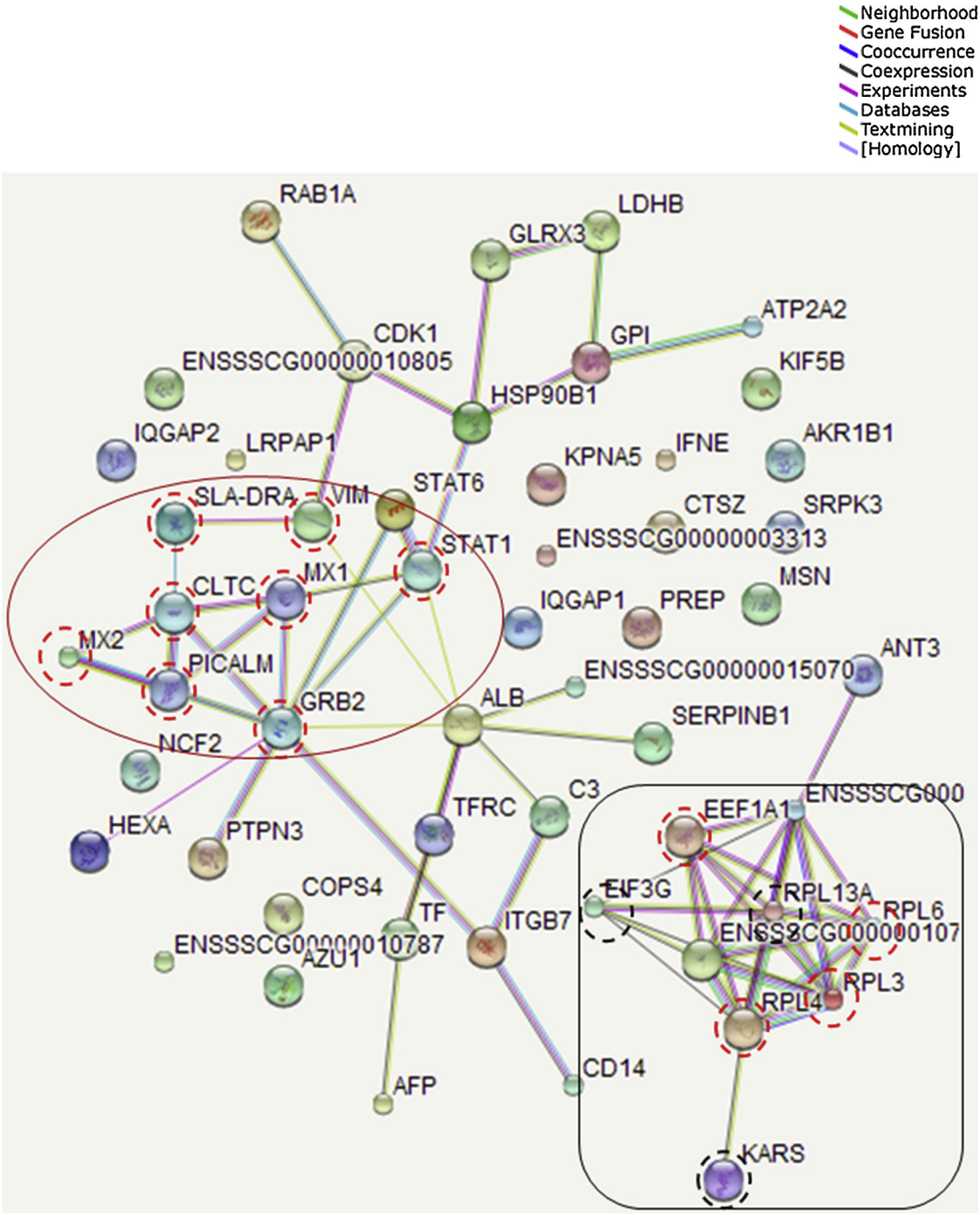

Fig. 6. The protein-protein interaction network analyzed by STRING software. An edge was drawn with up to 8 differently colored lines which represent the existence of the eight types of evidence used in predicting the associations. A green line indicates the presence of neighborhood evidence; a red line indicates gene fusion evidence; a blue line indicates co-occurrence evidence; a black line indicates co-expression evidence; a purple line indicates experimental evidence; a light blue line indicates database evidence; a yellow line indicates text mining evidence; a gray line indicates homology evidence. Red dotted circle means up-regulation; black dotted circle means down-regulation. Two concentrated protein regions were circled with red and squared with black respectively (For interpretation of the references to colour in this figure legend, the reader is referred to the web version of this article).

associated with the regulation of actin cytoskeleton were identified (Supplementary Fig. 3B and Supplementary Table 1). The expressions of these proteins such as IQGAP1 and IQGAP2 were significantly altered, which may affect the integrity and polymerization of actin cytoskeleton in PRRSV-infected MoDCs and then affect the function of MoDCs (Hedman et al., 2015; Magill et al., 2016).

MHC class II molecules as hallmark of APCs seem to be the first obvious candidate receptor for antigen delivery. Antibodies bound to MHC class II molecules were endocytosed and presented as antigens to lymphocytes (Alvarez et al., 2013). The potential of delivering antigens to MHC class II molecules was tested by using a recombinant single chain Fv fragment protein (scFv) specific to SLA-DR (Argilaguet et al., 2011). There were reports that observed no changes (Silva-Campa et al., 2010) or a reduction (Xiao et al., 2015; Flores-Mendoza et al., 2008; Park et al., 2008) or an increase (Rodriguez-Gomez et al., 2015) of swine leukocyte antigen SLA-DR. The expression of SLA-DR was detected at different post infection times and the results were different in those reports. In our study, the expression of SLA-DR was

significantly increased at 12 hpi, but not at 24 hpi and 36 hpi. It was shown that the expression of SLA-DR was changed as infection time went on (Fig. 5 and Supplementary Table 1). Previous reports showed that MHC I was down-regulated in PRRSV-infected MoDCs or PAMs (Wang et al., 2007; Du et al., 2015). We hypothesize that PRRSV participates in the MHC II antigen processing pathway in MoDCs, which need to be further studied.

More interestingly, we found that many proteins involved in JAK-STAT signaling pathway were significantly altered following PRRSV infection (Supplementary Fig. 3D and Supplementary Table 1). As we know, upon JAK1 and tyrosine kinase 2 (Jak1/Tyk2)-mediated tyrosine phosphorylation, STAT1 and STAT2 heterodimerize. Then the heterodimer binds IFN regulatory factor 9 (IRF9) in the cytoplasm and forms ISGF3 before transferred to the nucleus (Patel et al., 2010). It was reported that PRRSV inhibits type I interferon signaling by blocking STAT1/STAT2 nuclear translocation, and the levels of STAT1 are similar in MARC-145 cells infected with PRRSV VR2385 or mock infected for 24 h and then treated with IFN-α for 8 h (Patel et al., 2010). In our study, we also found that the expression of STAT1 was similar between PRRSV-infected MoDCs and mock-infected MoDCs at 24 hpi, which was consistent with previous report by Patel et al. In addition, the expression of STAT1 was up-regulated in PRRSV-infected MoDCs at 12 hpi and hardly detected at 36 hpi, which was probably due to the cell viability of MoDCs and the protein characteristics of STAT1 in MoDCs (Fig. 5). ISGF3 sequence-specifically binds to an IFN-stimulated response element (ISRE) that is present in numerous type I IFN-stimulated genes (ISGs) like double-stranded RNA-dependent protein kinase R (PKR), 2′-5′-oligoadenylate synthetase (OAS), myxovirus resistance 1 (Mx1), many of which exhibit antiviral activity (Du et al., 2014a; Haller et al., 2015). For example, Mx1 protein belongs to the dynamin superfamily, which is involved in endocytosis and important for innate host defense against RNA viruses. The polymorphism in the porcine Mx1 promoter is associated with resistance to PRRSV infection (Li et al., 2015a,b). Interestingly, antiviral proteins Mx1, Mx2 and OAS2 were significantly increased in PRRSV-infected MoDCs in our study and the expression changes of Mx1 were further confirmed by Western blotting (Fig. 5 and Supplementary Table 1). PRRSV infecting MoDCs may activate JAK-STAT signaling pathway and then promote the expression of Mx1, which plays an important role in anti-PRRSV activity.

STRING is database resource dedicating to identify the protein-protein interactions, including both physical and functional associations (Szklarczyk et al., 2011). Our analysis provides an essential system-level understanding of cellular events that occur in MoDCs following PRRSV infection. In this study, the STRING analysis revealed functional links among proteins that were significantly altered after PRRSV infecting MoDCs. Proteins were mainly concentrated in two regions which were circled with red and squared with black, respectively. Proteins in red circle were all up-regulated following PRRSV infection, and there were three down-regulated proteins in black square (Fig. 6 and Supplementary Table 1). Of which, Vimentin, CLTC, Mx1 and Mx2 are associated with endocytosis; SLA-DRA is associated with antigen processing and presentation; STAT1 is associated with JAK-STAT signaling pathway; Mx1 and Mx2 also play an important role in antiviral activity (Li et al., 2015a,b; Wang et al., 2016). Ribosomes are cellular machines that are essential for protein synthesis. The biogenesis of ribosomes is a highly complex and energy consuming process that initiates in the nucleolus (Goudarzi and Lindstrom, 2016). In this study, RPL3, RPL4, RPL6 and RPL13 A were associated with ribosome, of which, RPL3, RPL4 and RPL6 were up-regulated while RPL13 A was down-regulated. EEF1A and EIF3G were associated with RNA transport, EEF1A was up-regulated but EIF3G was down-regulated. KARS was down-regulated in our study which was associated with Aminoacyl-tRNA biosytheses (Fig. 6 and Supplementary Table 1). Their precise roles during PRRSV infection require further investigation.

5. Conclusion

In summary, we first used the iTRAQ proteomic analysis to examine the cellular protein profiles involved in PRRSV infection in MoDCs. We unambiguously identified 252 significant differently expressed cellular proteins. The differently expressed proteins identified and their networks should provide a framework to elucidate the molecular mechanism by which the complex interaction between PRRSV and MoDCs to drive or suppress PRRSV replication in MoDCs and pigs.

Conflict of interest statement

The authors declare that there is no conflict of interest.

Acknowledgments

We thank Dr. Ping Jiang, Nanjing Agricultural University, China, to provide the PRRSV SY0608 strain. This work was supported by The National Key Research and Development Program of China (2016YFD0501505), Young Taishan Scholars (tsqn20161057), Agricultural Scientific and Technological Innovation Project of Shandong Academy of Agricultural Sciences (CXGC2016C07), the National Natural Science Foundation of China (31672609, 31702215).

Appendix A. Supplementary data

Supplementary material related to this article can be found, in the online version, at doi:https://doi.org/10.1016/j.vetmic.2018.11.016.

References

Alvarez, B., Poderoso, T., Alonso, F., Ezquerra, A., Domínguez, J., Revilla, C., 2013. Antigen targeting to APC: from mice to veterinary species. Dev. Comp. Immunol. 41, 153–163.

Argilaguet, J.M., Pérez-Martín, E., Gallardo, C., Salguero, F.J., Borrego, B., Lacasta, A., Accensi, F., Díaz, I., Nofrarías, M., Pujols, J., Blanco, E., Pérez-Filgueira, M., Escribano, J.M., Rodríguez, F., 2011. Enhancing DNA immunization by targeting ASFV antigens to SLA-II bearing cells. Vaccine 29, 5379–5385.

Balmelli, C., Steiner, E., Moulin, H., Peduto, N., Herrmann, B., Summerfield, A., McCullough, K., 2011. Porcine circovirus type 2 DNA influences cytoskeleton rearrangements in plasmacytoid and monocyte-derived dendritic cells. Immunology 132, 57–65.

Banchereau, J., Steinman, R.M., 1998. Dendritic cells and the control of immunity. Nature 392, 245–252.

Bonazzi, M., Cossart, P., 2006. Bacterial entry into cells: a role for the endocytic machinery. FEBS Lett. 580, 2962–2967.

Butler, J.E., Lager, K.M., Golde, W., Faaberg, K.S., Sinkora, M., Loving, C., Zhang, Y.I., 2014. Porcine reproductive and respiratory syndrome (PRRS): an immune dysregulatory pandemic. Immunol. Res. 59, 81–108.

Chand, R.J., Trible, B.R., Rowland, R.R., 2012. Pathogenesis of porcine reproductive and respiratory syndrome virus. Curr. Opin.Virol 2, 256–263.

Comrie, W.A., Li, S., Boyle, S., Burkhardt, J.K., 2015. The dendritic cell cytoskeleton promotes T cell adhesion and activation by constraining ICAM-1 mobility. J. Cell Biol. 208, 457–473.

Du, J., Ge, X., Liu, Y., Jiang, P., Wang, Z., Zhang, R., Zhou, L., Guo, X., Han, J., Yang, H., 2015. Targeting swine leukocyte antigen class I molecules for proteasomal degradation by the nsp1alpha replicase protein of the chinese highly pathogenic porcine reproductive and respiratory syndrome virus strain JXwn06. J. Virol. 90, 682–693.

Du, Y., Bi, J., Liu, J., Liu, X., Wu, X., Jiang, P., Yoo, D., Zhang, Y., Wu, J., Wan, R., Zhao, X., Guo, L., Sun, W., Cong, X., Chen, L., Wang, J., 2014a. $3C^{pro}$ of foot-and-mouth disease virus antagonizes the interferon signaling pathway by blocking STAT1/STAT2 nuclear translocation. J. Virol. 88, 4908–4920.

Du, Y., Lu, Y., Wang, X., Qi, J., Liu, J., Hu, Y., Li, F., Wu, J., Guo, L., Liu, J., Tao, H., Sun, W., Chen, L., Cong, X., Ren, S., Shi, J., Li, J., Wang, J., Huang, B., Wan, R., 2014b. Highly efficient expression of interleukin-2 under the control of rabbit β-globin intron II gene enhances protective immune responses of porcine reproductive and respiratory syndrome (PRRS) DNA vaccine in pigs. PLoS One 9, e90326.

Duan, X., Nauwynck, H.J., Pensaert, M.B., 1997. Virus quantification and identification of cellular targets in the lungs and lymphoid tissues of pigs at different time intervals after inoculation with porcine reproductive and respiratory syndrome virus (PRRSV). Vet. Microbiol. 56, 9–19.

Flores-Mendoza, L., Silva-Campa, E., Resendiz, M., Osorio, F.A., Hernandez, J., 2008. Porcine reproductive and respiratory syndrome virus infects mature porcine dendritic cells and up-regulates interleukin-10 production. Clin.Vaccine Immunol. 15, 720–725.

Goudarzi, K.M., Lindstrom, M.S., 2016. Role of ribosomal protein mutations in tumor development (Review). Int. J. Oncol. 48, 1314–1324.
Guo, X., Hu, H., Chen, F., Li, Z., Ye, S., Cheng, S., Zhang, M., He, Q., 2016. iTRAQ-based comparative proteomic analysis of Vero cells infected with virulent and CV777 vaccine strain-like strains of porcine epidemic diarrhea virus. J. Proteomics 130, 65–75.
Haller, O., Staeheli, P., Schwemmle, M., Kochs, G., 2015. Mx GTPases: dynamin-like antiviral machines of innate immunity. Trends Microbiol. 23, 154–163.
Hedman, A.C., Smith, J.M., Sacks, D.B., 2015. The biology of IQGAP proteins: beyond the cytoskeleton. EMBO Rep. 16, 427–446.
Hu, Y., Cong, X.Y., Chen, L., Qi, J., Wu, X.J., Zhou, M.M., Yoo, D.W., Li, F., Sun, W.B., Zhao, X.M., Chen, Z., Yu, J., Du, Y.J., Wang, J.B., 2016. Synergy of TLR3 and 7 ligands significanty enhances function of DCs to present inactivated PRRSV antigen through TRIF/MyD88-NF-Kb signaling pathay. Sci. Rep. 6, 23977.
Lawson, S.R., Rossow, K.D., Collins, J.E., Benfield, D.A., Rowland, R.R., 1997. Porcine reproductive and respiratory syndrome virus infection of gnotobiotic pigs sites of virus replication and co-localization with MAC-387 staining at 21 days post-infection. Virus Res. 51, 105–113.
Lemire, P., Houde, M., Segura, M., 2012. Encapsulated group B Streptococcus modulates dendritic cell functions via lipid rafts and clathrin-mediated endocytosis. Cell. Microbiol. 14, 1707–1719.
Li, X., Wang, Q., Gao, Y., Qi, X., Wang, Y., Gao, H., Wang, X., 2015a. Quantitative iTRAQ LC-MS/MS proteomics reveals the proteome profiles of DF-1 cells after infection with subgroup J Avian leukosis virus. Biomed Res. Int., 395307.
Li, Y., Liang, S., Liu, H., Sun, Y., Kang, L., Jiang, Y., 2015b. Identification of a short interspersed repetitive element insertion polymorphism in the porcine MX1 promoter associated with resistance to porcine reproductive and respiratory syndrome virus infection. Anim. Genet. 46, 437–440.
Li, Y., Wang, X., Bo, K., Wang, X., Tang, B., Yang, B., Jiang, W., Jiang, P., 2007. Emergence of a highly pathogenic porcine reproductive and respiratory syndrome virus in the Mid-Eastern region of China. Vet. J. 174, 577–584.
Liu, J., Bai, J., Lu, Q., Zhang, L., Jiang, Z., Michal, J.J., He, Q., Jiang, P., 2013. Two-dimensional liquid chromatography-tandem mass spectrometry coupled with isobaric tags for relative and absolute quantification (iTRAQ) labeling approach revealed first proteome profiles of pulmonary alveolar macrophages infected with porcine circovirus type 2. J. Proteomics 79, 72–86.
Lu, Q., Bai, J., Zhang, L., Liu, J., Jiang, Z., Michal, J.J., He, Q., Jiang, P., 2012. Two-dimensional liquid chromatography-tandem mass spectrometry coupled with isobaric tags for relative and absolute quantification (iTRAQ) labeling approach revealed first proteome profiles of pulmonary alveolar macrophages infected with porcine reproductive and respiratory syndrome virus. J. Proteome Res. 11, 2890–2903.
Magill, D.J., Hamilton, E., Shirran, S.L., Botting, C.H., Timson, D.J., 2016. On the interaction between human IQGAP1 and actin. Protein Pept. Lett. 23, 386–395.
McMahon, H.T., Boucrot, E., 2011. Molecular mechanism and physiological functions of clathrin-mediated endocytosis. Nat. Rev. Mol. Cell Bio. 12, 517–533.
Meulenberg, J.J.M., 2000. PRRSV, the virus. Vet. Res. 31, 11–21.
Park, J.Y., Kim, H.S., Seo, S.H., 2008. Characterization of interaction between porcine reproductive and respiratory syndrome virus and porcine dendritic cells. J. Microbiol. Biotechnol. 18, 1709–1716.
Patel, D., Nan, Y., Shen, M., Ritthipichai, K., Zhu, X., Zhang, Y.J., 2010. Porcine reproductive and respiratory syndrome virus inhibits type I interferon signaling by blocking STAT1/STAT2 nuclear translocation. J. Virol. 84, 11045–11055.
Rodriguez-Gomez, I.M., Kaser, T., Gomez-Laguna, J., Lamp, B., Sinn, L., Rumenapf, T., Carrasco, L., Saalmuller, A., Gerner, W., 2015. PRRSV-infected monocyte-derived dendritic cells express high levels of SLA-DR and CD80/86 but do not stimulate PRRSV-naive regulatory T cells to proliferate. Vet. Res. 46, 54.
Shi, C., Liu, Y., Ding, Y., Zhang, Y., Zhang, J., 2015. PRRSV receptors and their roles in virus infection. Arch. Microbiol. 197, 503–512.
Silva-Campa, E., Cordoba, L., Fraile, L., Flores-Mendoza, L., Montoya, M., Hernandez, J., 2010. European genotype of porcine reproductive and respiratory syndrome (PRRSV) infects monocyte-derived dendritic cells but does not induce Treg cells. Virology. 396, 264–271.
Summerfield, A., McCullough, K.C., 2009. The porcine dendritic cell family. Dev. Com. immunol. 33, 299–309.
Szklarczyk, D., Franceschini, A., Kuhn, M., Simonovic, M., Roth, A., Minguez, P., Doerks, T., Stark, M., Muller, J., Bork, P., Jensen, L.J., von Mering, C., 2011. The STRING database in 2011: functional interaction networks of proteins, globally integrated and scored. Nucleic Acids Res. 39, D561–568.
Tebar, F., Bohlander, S.K., Sorkin, A., 1999. Clathrin assembly lymphoid myeloid leukemia (CALM) protein: localization in endocytic-coated pits, interactions with clathrin, and the impact of overexpression on clathrin-mediated traffic. Mol. Biol. Cell 10, 2687–2702.
Van, B.W., Delputte, P.L., Van, G.H., Misinzo, G., Vanderheijden, N., Duan, X., Nauwynck, H.J., 2010. Porcine reproductive and respiratory syndrome virus entry into the porcine macrophage. J. Gen. Virol. 91, 1659–1667.
Wang, H., Bai, J., Fan, B., Li, Y., Zhang, Q., Jiang, P., 2016. The interferon-induced Mx2 inhibits porcine reproductive and respiratory syndrome virus replication. J. Interferon Cytokine Res. 36, 129–139.
Wang, J.H., Wells, C., Wu, L., 2008. Macropinocytosis and cytoskeleton contribute to dendritic cell-mediated HIV-1 transmission to CD4+ T cells. Virology 381, 143–154.
Wang, X., Eaton, M., Mayer, M., Li, H., He, D., Nelson, E., Christopher-Hennings, J., 2007. Porcine reproductive and respiratory syndrome virus productively infects monocyte-derived dendritic cells and compromises their antigen-presenting ability. Arch. Virol. 152, 289–303.
West, M.A., Wallin, R.P., Matthews, S.P., Svensson, H.G., Zaru, R., Ljunggren, H.G., Prescott, A.R., Watts, C., 2004. Enhanced DC antigen capture via TLR induced actin-remodeling. Science. 305, 1153–1157.
Xiao, Y., An, T.Q., Tian, Z.J., Wei, T.C., Jiang, Y.F., Peng, J.M., Zhou, Y.J., Cai, X.H., Tong, G.Z., 2015. The gene expression profile of porcine alveolar macrophages infected with a highly pathogenic porcine reproductive and respiratory syndrome virus indicates overstimulation of the innate immune system by the virus. Arch. Virol. 160, 649–662.
Yang, Y., Liu, W., Yan, G., Luo, Y., Zhao, J., Yang, X., Mei, M., Wu, X., Guo, X., 2015. iTRAQ protein profile analysis of neuroblastoma (NA) cells infected with the rabies viruses rHep-Flury and Hep-dG. Front. Microbiol. 6, 691.
Yang, Y., Ma, L., Zeng, H., Chen, L.Y., Zheng, Y., Li, C.X., Yang, Z.P., Wu, N., Mu, X., Dai, C.Y., Guan, H.L., Cui, X.M., Liu, Y., 2018. iTRAQ-based proteomics screen for potential regulators of wheat (Triticum aestivum L.) root cell wall component response to Al stress. Gene. 675, 301–311.
Ye, F., Xin, Z., Han, W., Fan, J., Yin, B., Wu, S., Yang, W., Yuan, J., Qiang, B., Sun, W., Peng, X., 2015. Quantitative Proteomics Analysis of the Hepatitis C Virus Replicon High-Permissive and Low-Permissive Cell Lines. PLoS One 10, e0142082.
Zeng, S., Zhang, H., Ding, Z., Luo, R., An, K., Liu, L., Bi, J., Chen, H., Xiao, S., Fang, L., 2015. Proteome analysis of porcine epidemic diarrhea virus (PEDV)-infected Vero cells. Proteomics 15, 1819–1828.
Zhang, P., Zhu, S., Zhao, M., Zhao, P., Zhao, H., Deng, J., Li, J., 2018. Identification of plasma biomarkers for diffuse axonal injury in rats by iTRAQ-coupled LC-MS/MS and bioinformatics analysis. Brain Res. Bull. 142, 224–232.
Zhang, Q., Yoo, D., 2015. PRRS virus receptors and their role for pathogenesis. Vet. Microbiol. 177, 229–241.
Zhu, Z., Yang, F., Zhang, K., Cao, W., Jin, Y., Wang, G., Mao, R., Li, D., Guo, J., Liu, X., Zheng, H., 2015. Comparative Proteomic Analysis of Wild-Type and SAP Domain Mutant Foot-and-Mouth Disease Virus-Infected Porcine Cells Identifies the Ubiquitin-Activating Enzyme UBE1 Required for Virus Replication. J. Proteome Res. 14, 4194–4206.